Title

A GCM investigation of impact of aerosols on the precipitation in Amazon during the dry to wet transition

Journal

Climate Dynamics, 48(7-8)

ISSN

0930-7575

Authors

Gu, Yu
Liou, KN
Jiang, JH
et al.

Publication Date

2017-04-01

DOI

10.1007/s00382-016-3211-7

Peer reviewed

Clim Dyn (2017) 48:2393–2404
DOI 10.1007/s00382-016-3211-7

A GCM investigation of impact of aerosols on the precipitation in Amazon during the dry to wet transition

Yu Gu[1] · K. N. Liou[1] · J. H. Jiang[2] · R. Fu[3] · Sarah Lu[4] · Y. Xue[5]

Received: 19 January 2016 / Accepted: 28 May 2016 / Published online: 9 June 2016

Abstract The climatic effects of aerosols on the precipitation over the Amazon during the dry to wet transition period have been investigated using an atmospheric general circulation model, NCEP/AGCM, and the aerosol climatology data. We found increased instability during the dry season and delayed wet season onset with aerosols included in the model simulation, leading to the delay of the maximum precipitation over the Amazon by about half a month. In particular, our GCM simulations show that surface solar flux is reduced in the Amazon due to the absorption and scattering of the solar radiation by aerosols, leading to decreased surface temperature. Reduced surface solar flux is balanced by decreases in both surface sensible heat and latent heat fluxes. During the wet season, the subtropical system over the Amazon has a shallower convection. With the inclusion of aerosols in the simulation, precipitation in the rainy season over the Amazon decreases in the major rainfall band, which partially corrects the overestimate of the simulated precipitation in that region. The reduced surface temperature by aerosols is also coupled with a warming in the middle troposphere, leading to increased atmosphere stability and moisture divergence over the Amazon. However, during the dry season when the convective system is stronger over the Amazon, rainfall increases in that region due to the warming of the air over the upper troposphere produced by biomass burning aerosols, which produces an anomalous upward motion and a convergence of moisture flux over the Amazon and draws the moisture and precipitation further inland. Therefore, aerosol effects on precipitation depend on the large-scale atmospheric stability, resulting in their different roles over the Amazon during the dry and wet seasons.

✉ Yu Gu
gu@atmos.ucla.edu

[1] Department of Atmospheric and Oceanic Science, Joint Institute for Regional Earth System Science and Engineering, University of California, Los Angeles, CA 90095, USA

[2] Jet Propulsion Laboratory, California Institute of Technology, Pasadena, CA, USA

[3] Jackson School of Geosciences, University of Texas at Austin, Austin, TX, USA

[4] University at Albany, State University of New York, Albany, NY, USA

[5] Department of Geography, University of California, Los Angeles, CA 90095, USA

1 Introduction

The Amazon has been experiencing worsened drought during the past decade. The 2005 drought in the Amazon was described as a "once a century" event (Marengo et al. 2008), but it was followed by an even worse one only 5 years later in 2010 (Lewis et al. 2011). The droughts were likely associated with unusually warm seas in the Atlantic Ocean off the Brazilian coast, the possible result of anthropogenic emissions. Using monthly data from simulations performed by global climate models of the Coupled Model Comparison Project, scientists have found that in a warming planet, the dry season of the Amazon would begin earlier in the year and end later in the year, making its overall impact more marked (Boisier et al. 2015). The variability of the rainy season onset over the Amazon has been attributed by most studies to the variability of the tropical oceans, such as El Nino-Southern Oscillation (ENSO) and anomalies in the north–south gradient of the tropical Atlantic sea surface temperature (SST; Liebmann and Marengo 2001; Fu et al. 2001; Zeng et al. 2008; Cox et al. 2008; Marengo

et al. 2011), and land surface conditions (Fu and Li 2004; Butt et al. 2011). While these are very important factors, whether they can explain the observed climate variability of the rainy season onset or the length of the dry season remains unclear. Evidences of significant aerosol influence on precipitation in Amazon (e.g. Martins et al. 2009; Jiang et al. 2008) and other places in the world (e.g. Gu et al. 2006, 2012, 2016) are emerging, raising the question as to whether or not aerosol could contribute to the drought in the Amazon.

The typical dry (June to November) to wet (December to May) circulation transition in the Amazon is largely determined by the elevated diabatic heating produced by convection (e.g., Lenters and Cook 1997), either locally generated or propagating as a meso-scale system (Greco et al. 1990; Machado et al. 1998). The dry season in the Amazon is characterized by the deeper propagating convection (Silva Dias 2002; Rickenbach 2002; Petersen et al. 2002, 2006) with warmer surface temperature and strong vertical wind shear, convective available energy (CAPE) and inhibition energy (CIN). During the wet season, however, the atmosphere is thermodynamically near neutral with cooler surface temperature, shallower convection, and weaker wind shear, CAPE and CIN. Since the atmospheric thermodynamic structure is generally near neutrally stable during the transition, relatively small changes in the atmospheric boundary layer due to changes of land surface fluxes, clouds and aerosols, during the early phase of the dry to wet transition, could induce a chain of feedbacks, leading to the reversal of large scale wind and moisture transport during the transition (Li and Fu 2004). The aerosol loadings are strongest at the initial phase of the transition, while the influence by ENSO and Atlantic variability are relatively weak during June–August so that the aerosols can play a more important role in the early transition of the atmospheric thermodynamic structure, as indicated by the observed strong links between aerosol optical depth during dry season and subsequent changes of rainy season onset (e.g., Fu and Li 2004). Once the large-scale transition begins, aerosol concentrations decrease and remotely forced large-scale atmospheric circulation, such as ENSO, becomes the dominant source of rainfall variability (Marengo et al. 2008).

Aerosols from pasture and fires spread over a large area of the Amazon (Martin et al. 2010), in which biomass burning aerosols dominate. These absorbing aerosols can alter the radiation budget at the top of the atmosphere and the surface, and also influence the cloud formation, regional circulation, and precipitation through direct, semi-direct, and indirect effects. Understanding the impact of aerosols on radiation, clouds, and precipitation in the Amazon is a key to reducing uncertainties in climate change simulations. The direct and semi-direct effects are related to the high absorption of biomass burning aerosols (Gu et al. 2006, 2012). These aerosols substantially absorb the incoming sunlight and hence influence the radiation field, referred to as the direct radiative effect. The direct effect would heat the air column and modify the horizontal and vertical temperature gradients, atmospheric stability, and convection strength (Miller and Tegen 1998; Menon et al. 2002; Gu et al. 2006). Meanwhile, due to the heating of the air column by biomass burning aerosols, the cloud field can be modified and hence exert cloud radiative forcing, referred to as the semi-direct effect (Hansen et al. 1997; Gu et al. 2010). Absorbing aerosols within the cloud may decrease cloud cover by heating the air and reducing relative humidity. However, when absorbing aerosols are located above the cloud and increase the temperature there, they may enhance the cloud development by the suppression of diffusion from entrainment (Johnson et al. 2004). When biomass burning aerosols are present in the cloudy atmosphere, they can serve as cloud condensation nuclei (CCN) or ice nuclei (IN), leading to increased cloud particle number. Consequently, the cloud particle size decreases (e.g. Jiang et al. 2011) and could alter cloud lifetime and cloud radiative forcing. This process is known as the first indirect effect since it is through the modification of cloud fields due to changes in CCNs or INs associated with aerosols (Gu et al. 2012).

A number of studies have been conducted to investigate the influence of biomass burning aerosols on precipitation over the Amazon (e.g., Jiang et al. 2008; Martins et al. 2009; Goncalves et al. 2015), focusing more on aerosol indirect effect. Using satellite observations, Jiang et al. (2008) found the aerosol polluted clouds during dry season in Amazon have significantly weaker precipitation than those from the clean clouds. Using a regional climate model in a case study, Martins et al. (2009) found that higher CCN concentrations increased high rainfall rates but reduced low-to-moderate rainfall rates. This is because that the aerosol indirect effect resulted in decreased cloud cover, allowing more solar radiation to be available in the lower atmosphere. Aerosol absorption in the lower layers delayed the convective evolution but produced higher maximum rainfall rates due to increased instability. Using observations from an S-band radar in the Amazon and in situ measurements of biomass burning aerosol, Goncalves et al. (2015) found that the influence of aerosol on precipitation is modulated by the atmospheric instability. For more stable atmospheres (wet season), the higher the aerosol concentration is, the lower the precipitation is over the region. On the other hand, for more unstable cases (dry season), higher concentrations of black carbon are associated with greater precipitation. However, they pointed out that due to limitations imposed by the available data set, the responsible mechanisms need to be clarified by climate

model simulations. Recently, Gu et al. (2016) have found that the dust aerosol effects on precipitation over the North Africa and over South/East Asia show very different characteristics, in part due to the different large-scale circulation patterns and convection strength.

The purpose of this study is to investigate how the aerosols influence the radiation, convection, clouds, and precipitation during the early phase of the dry to wet transition over the Amazon by examining the responses of the regional climate system to direct and semi-direct aerosol radiative forcing in the National Centers for Environmental Prediction (NCEP) Atmospheric General Circulation Model (AGCM). The organization of this paper is as follows. In Sect. 2, we present the model employed including the treatment of aerosols in the radiation calculations and the AGCM experiment design. The model simulations and discussions are presented in Sect. 3. Conclusions are given in Sect. 4.

2 Model description

The NCEP AGCM (Kanamitsu et al. 2002) with a horizontal resolution T62 and 17 vertical levels was used in this study. T62 represents 92 longitude equally spaced and 94 latitude unequally spaced grid points, with a horizontal resolution of approximate 1.875° × 1.90° at the equator. The prognostic cloud water and ice mixing ratios have two sources, namely grid-scale condensation (Zhao and Carr 1997; Sundqvist et al. 1989) and convection (Pan and Wu 1995). Both of them produce either cloud water or cloud ice, depending on the cloud substance at and above the grid point and the temperature. Evaporation of cloud occurs when the relative humidity is lower than the critical value required for condensation. Precipitation is diagnostically calculated directly from the cloud water/ice mixing ratio. The fractional cloud cover used in the radiation calculation is diagnostically determined by the predicted cloud condensate based on the approach of Xu and Randall (1996). The model also has ozone as a prognostic variable with a simple parameterization for ozone production and destruction based on 10-day mean climatological data available from NASA/GSFC. The shortwave radiation is parameterized following the NASA approach (Chou et al. 1998; Hou et al. 1996, 2002) and the longwave radiation following the GFDL scheme (Fels and Schwarzkopf 1975; Schwarzkopf and Fels 1991). For radiation calculation associated with clouds, multiple scattering is treated using a delta-Eddington approximation with a two-stream adding method (Joseph et al. 1976; Coakley et al. 1983). Cloud single-scattering properties are parameterized as a function of effective radius of the cloud condensate. For liquid water cloud, an effective radius of 5 μm is used for temperature above 273.16 K, and a value between 5 and 10 μm is used for supercooled water with temperature between melting point and 253.16 K (Kiehl et al. 1998). The effective radius for ice is parameterized as a linear function of temperature, ranging from a value of 80 μm at 163.17 K to 20 μm at temperature at or below 223.16 K (Heymsfield and McFarquhar 1996). Both radiation parameterizations use random cloud overlap with shortwave and longwave being called every 1 and 3 h, respectively. The Simplified Simple Biosphere Model version 2 (SSiB2) has been coupled with this AGCM (Xue et al. 1991, 2004; Zhan et al. 2003) and used in this study, along with the climatological sea surface temperature (SST).

A tropospheric climatological aerosol distribution at 5-degree resolution (Hess et al. 1998) is used in radiation calculations. Seven aerosol vertical distribution profiles are used in the data set. For each profile, up to five distinct vertical atmospheric domains are given according to the geographic region and the type of profile selected. Ten different types of aerosol components are used in the construction of the aerosol profiles, including water-insoluble, soot, four modes of mineral dust (nucleation, accumulation, coarse, and transported modes), water-soluble, two modes of sea salt (accumulation and coarse modes), and sulfate. For each grid point, climatological data of aerosol components are given, including the aerosol profile type, the mixing ratio of the aerosol components, and the mean particle number density. A separate stratospheric volcanic aerosol scheme was also added that is capable of handling volcanic eruption events. A generalized spectral mapping scheme was developed to compute aerosol optical properties at each radiation spectral band.

Two sets of sensitivity experiments have been carried out as described below. Each simulation is a 6-year run with the initial condition corresponding to January 1, 2006. Note that each experiment contains 6 years of integration with prescribed climatological SST and land processes, representing six members starting from different initial conditions.

1. Case CTRL: In the control run (CTRL), the aerosol is turned off, therefore the aerosol effect is excluded from model simulation.
2. Case AERO: In the second experiment, the aerosol effect is accounted for by incorporating the climatology aerosol data in NCEP AGCM.

Results are presented in ensemble means of each set of experiment. Since the two sets of experiments are identical except for the aerosols, significant differences in the ensemble mean between the two sets of experiments can be attributed to the sensitivity of the regional climate responses to aerosol radiative forcing. The two-tailed Student's *t* test, in

which deviations of the estimated parameter in either direction are considered theoretically possible, is used in this study to measure the statistical significance of the sensitivity simulations. The threshold chosen for statistical significance is 0.1 for all the results in this study.

3 Model simulations

3.1 General features and evolution of the South America monsoon

Figure 1a shows the December–February (DJF) mean precipitation over the Amazon obtained from the Climate Prediction Center Merged Analysis of Precipitation (CMAP; Xie and Arkin 1997) in which observations from the rain gauge are merged with several satellite-based observations. The major South America monsoon rainfall band is located in the region between 5°N–25°S and 70°W–40°W (Fig. 1a). The CTRL experiment simulated DJF precipitation reasonably well, with the South America monsoon precipitation captured, albeit the western Amazon along the Andes was dry and too much precipitation was simulated over the central and eastern Amazon (Fig. 1b). Compared to CTRL, AERO, with the inclusion of aerosols in the simulation, improved the simulation by reducing the precipitation in the central and eastern Amazon while enhancing the rainfall in the western Amazon. Here dots represent differences that are statistically significant at a significance level of 0.1 (Fig. 1c).

Figure 2 illustrates the South America monsoon evolution in the form of monthly mean precipitation maps for August, October, December, and February. In August which is the middle of the dry season of the Amazon, the observed rainfall band is mainly located over equator—15°N, to the north of Amazon (Fig. 2a), with local maxima over the Caribbean coast of Venezuela, Columbia, and Guyana, while the Amazon region was very dry. The CTRL well simulated these features; however, the simulated precipitation maximum was higher compared to CMAP (Fig. 2e). During the early phase of the dry to wet transition, a southeastward shift of the convection from the equator toward the Amazon basin and the Brazilian high lands is observed in CMAP. Besides the precipitation center over the equator to 15°N, the October mean precipitation also shows a maximum precipitation (4–6 mm/day) over the central Amazon (Fig. 2b). The CTRL captured the southeastern spreading of the precipitation and a dry northeastern Brazil in October. The simulated precipitation over the Andes, however, was stronger than that in CMAP, and the maximum over the central Amazon was missing (Fig. 2f). The maximum precipitation extends toward the southeast in December (Fig. 2c). The CTRL showed the observed extension of rainfall into southeastern South America and the heavy rainfall in the central Amazon and southeastern Brazil. The simulated precipitation, however, was much heavier over the monsoon region. In addition, the simulated precipitation also showed a strong branch along the northeast South American coast, which merged with the ITCZ (Fig. 2g). In CMAP observations, however, there is

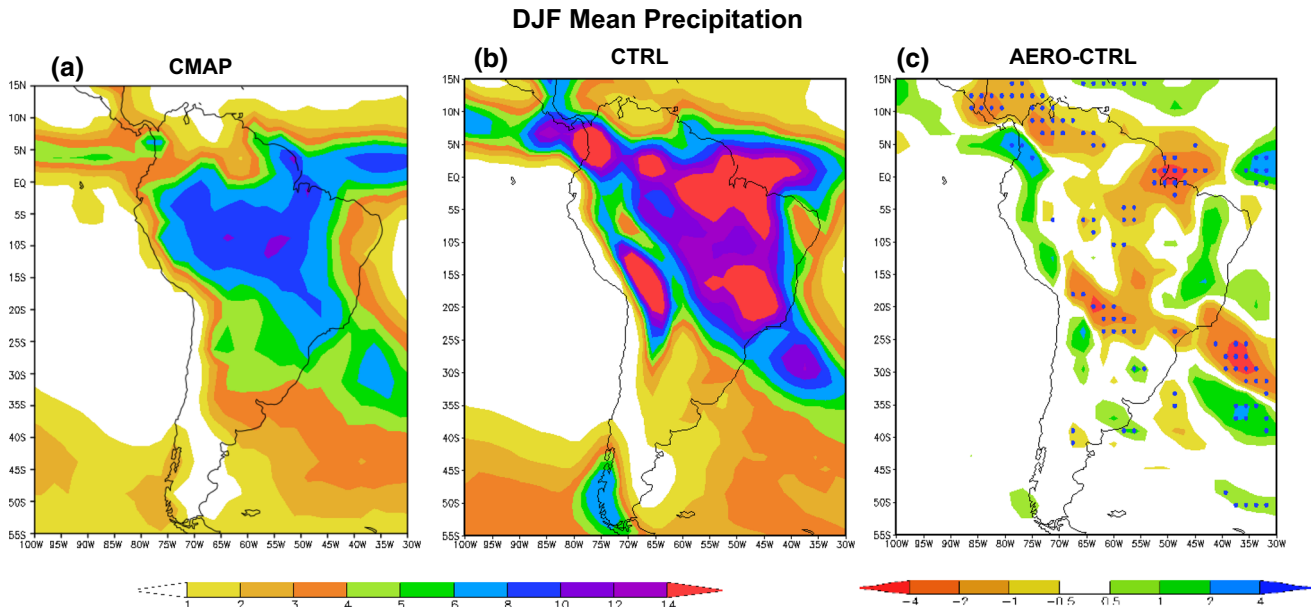

Fig. 1 DJF mean precipitation (mm day^{-1}). **a** Observations from CMAP, **b** simulated from CTRL, and **c** differences between AERO and CTRL over Amazon. *The dotted areas* denote differences which are statistically significant at a significance level of 0.1

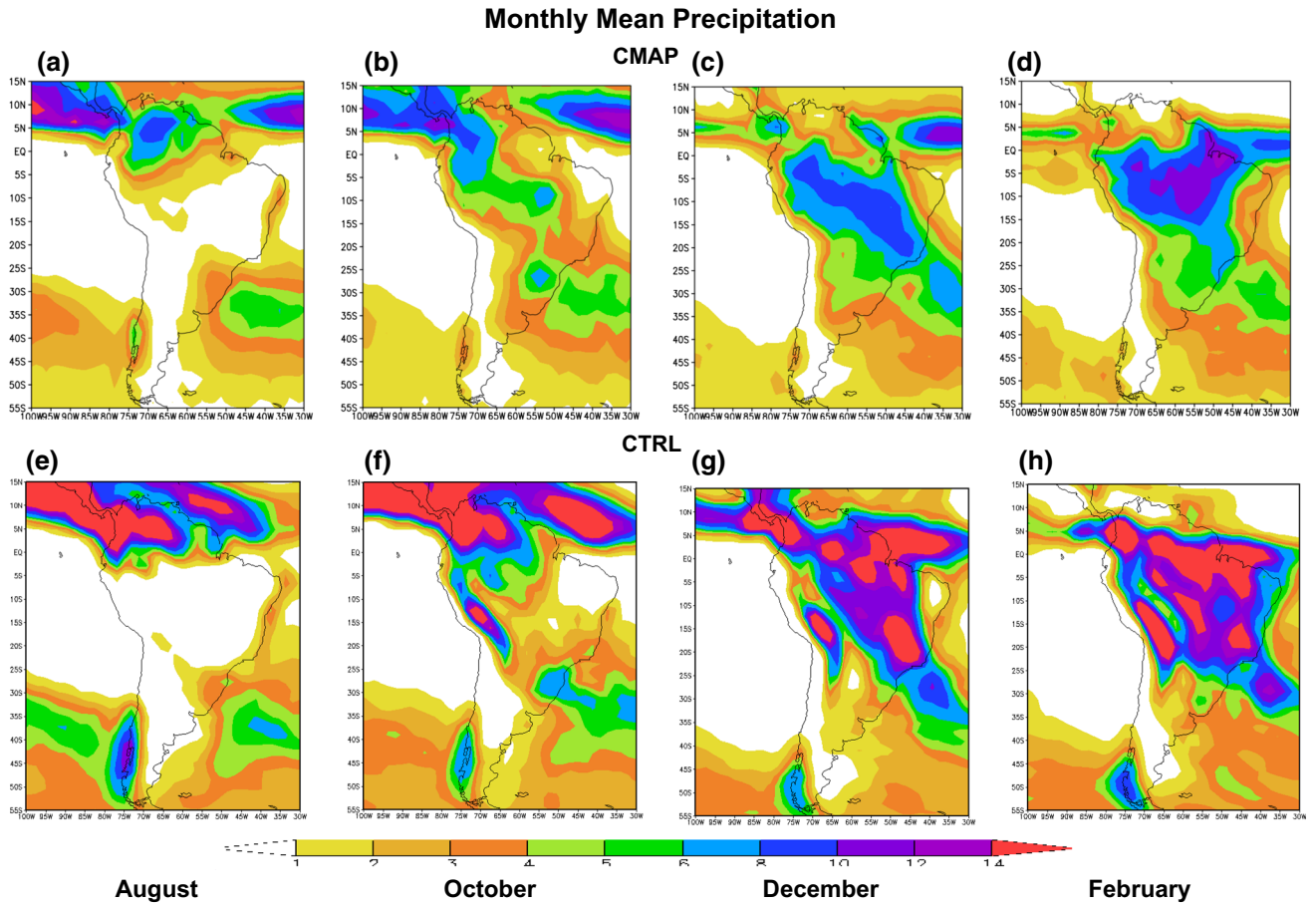

Fig. 2 Monthly mean precipitation (mm day^{-1}) from CMAP observations (*top panel*) for **a** August, **b** October, **c** December, and **d** February, and simulated from CTRL for **e** August, **f** October, **g** December, and **h** February over Amazon

a clear separation between the monsoon region over the land and the ITCZ over the Atlantic Ocean (Fig. 2c). During the mature phase of the South American monsoon, the convection gradually retreats northward toward the equator, merging with the ITCZ. In February, the major precipitation band occurs along the equator (Fig. 2d). These features were well simulated in the CTRL. The intensity, however, was stronger over the monsoon region. Heavy rain was also found along the Andes, which is not seen in the observation (Fig. 2h).

3.2 Aerosol effects

The aerosol effect can be shown by examining the differences between cases AERO and CTRL. It is shown from Fig. 1c that due to the aerosol's effect, precipitation in the wet season decreases in this major rainfall band, where aerosols are located, which partially corrects the overestimate of the simulated precipitation in that region. In order to see the aerosol effect in the dry to wet transition, Fig. 3 shows the temporal revolution of monthly rainfall for AERO and CTRL averaged over 50°W–70°W from January to December. It is found that during the late phase of dry season, the major rainfall band over 10°N to equator was weakened over October–November, while precipitation was enhanced over the southern Amazon due to the aerosol effect. During the wet season, the maximum precipitation over the Amazon started to occur between January and February in the CTRL (Fig. 3a). However, it occurred around February in the case AERO (Fig. 3b), indicating that aerosol effect tends to delay the maximum precipitation over the Amazon by about half a month.

Figure 4 shows the temporal evolution of the zonally averaged (50°W–70°W) differences in precipitation, cloud cover, surface downward solar flux, OLR, sensible heat flux, and latent heat flux. Precipitation generally decreased over the Amazon in the wet season during December to February (Fig. 4a), but increased in March, corresponding to the decreased/increased cloud cover (Fig. 4b), indicating the delay of the wet season over the Amazon in association with aerosols. Surface solar flux decreased in the whole area due to the absorption and scattering of the solar

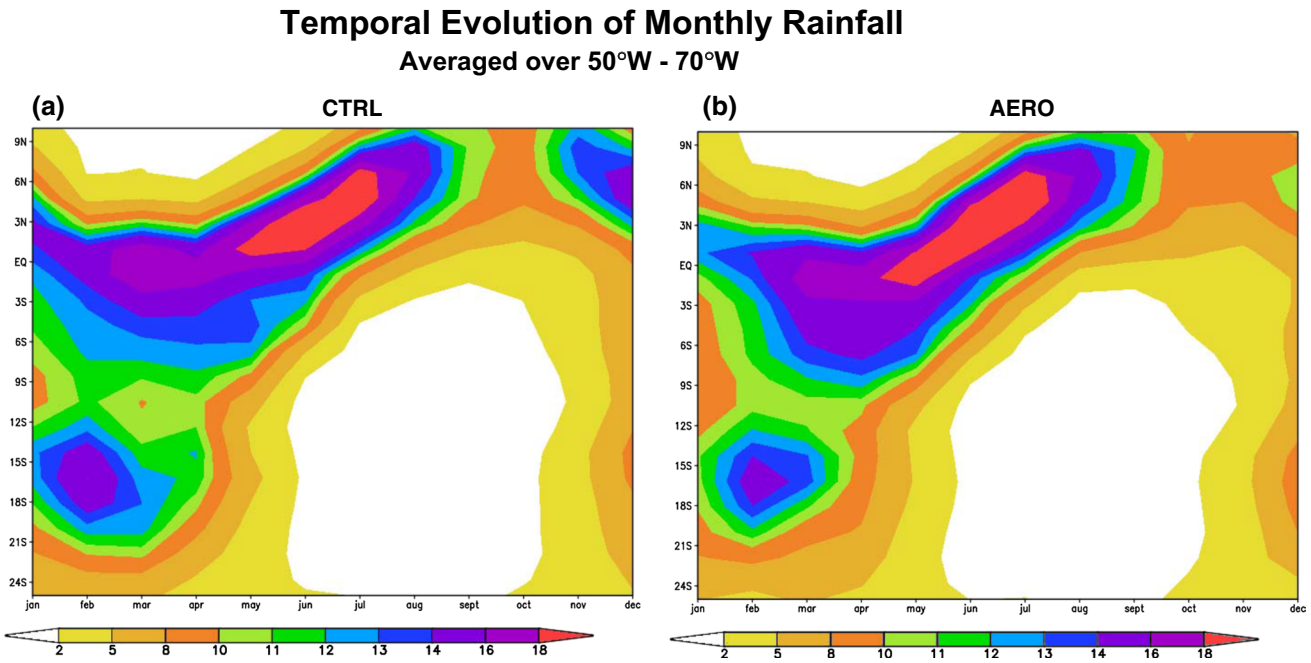

Fig. 3 Temporal evolution of monthly mean precipitation (mm day^{-1}) averaged over 50°W–70°W simulated from **a** CTRL and **b** AERO

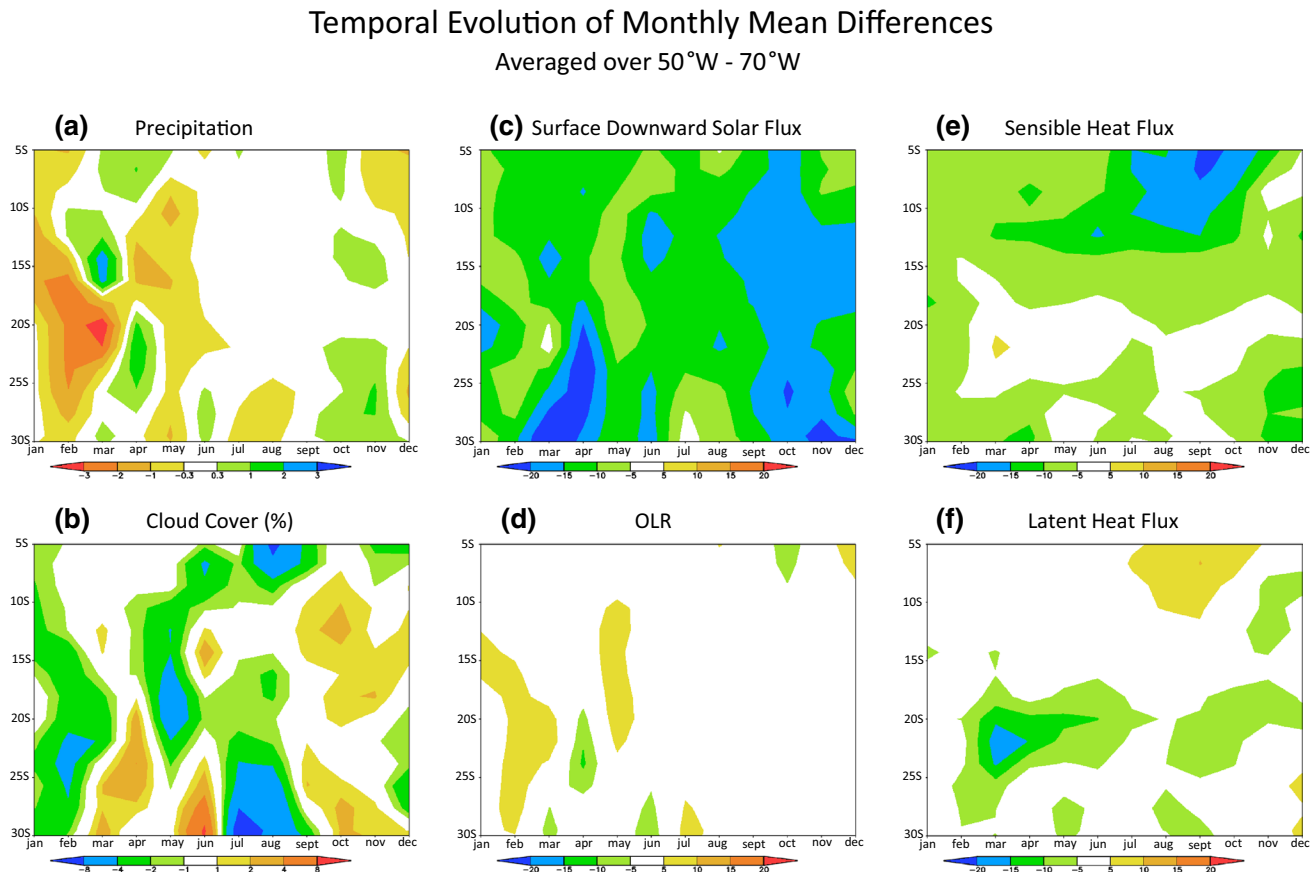

Fig. 4 Temporal evolution of monthly mean differences between AERO and CTRL averaged over 50°W–70°W in **a** precipitation (mm day^{-1}), **b** cloud cover (%), **c** surface downward solar flux (W m^{-2}), **d** OLR (W m^{-2}), **e** sensible heat flux (W m^{-2}), and **f** latent heat flux (W m^{-2})

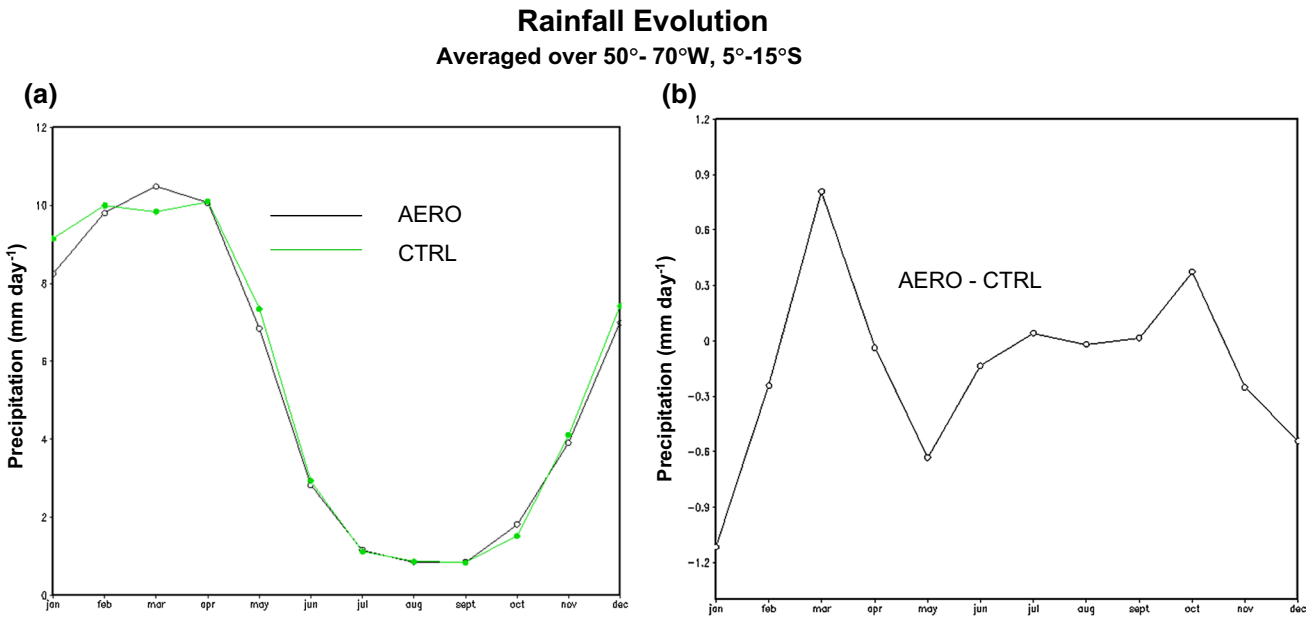

Fig. 5 Domain averaged precipitation evolution over 50°W–70°W, 5°S–15°S for **a** CTRL and AERO, and **b** their differences

radiation by aerosols. The larger reductions in March and October–November were due to the increased cloud cover (Fig. 4c). Outgoing longwave radiation (OLR) is an indication of convection strength. Increased/decreased OLR corresponded to weakened/strengthened convection and hence reduced/enhanced precipitation, as shown in Fig. 4d for January–February/March. Sensible heat flux showed decreases over the region due to the decreased surface temperature caused by the aerosols (Fig. 4e). Latent heat also decreased over the Southern Amazon in response to the reduced precipitation and surface solar radiation (Fig. 4f). Figure 5 further illustrates the rainfall evolution over the Amazon by showing the domain averaged (50°W–70°W, 5°S–15°S) precipitation for CTRL and AERO cases (Fig. 5a) and their differences (Fig. 5b). It is shown that due to the aerosol effect, the domain averaged precipitation was reduced during December–February while enhanced in October and March, indicating the increase/decrease of precipitation in dry/wet season and the delays of the onset of the wet season and the maximum of the rainfall.

Since we focus on the aerosol effect during the transition period, Fig. 6 shows the differences in precipitation in October (late phase of dry season) and December (early phase of wet season), respectively. In October, the observed major rainfall band is located over 0°N–15°N with another maximum over the central Amazon (Fig. 2b) where the CTRL overestimate the precipitation in the major rainfall band but underestimate the rainfall over the central Amazon (Fig. 2f). With aerosol effect included in the simulation, the precipitation was weakened over the major rainfall band but strengthened over the central Amazon (Fig. 6a). In December the major rainfall band shifts to the central Amazon (Fig. 2c), where the precipitation was overestimated in the CTRL (Fig. 2g). The effects of aerosol led to decreases in precipitation over the Amazon (Fig. 6b). Therefore, aerosol effect generally leads to less precipitation over the major rainfall band. However, for the Amazon region where the aerosols are located, precipitation increases in the dry season but decreases in the wet season. When the atmosphere over the Amazon is more unstable in the dry season, biomass burning aerosols can draw the precipitation further inland to the Amazon area, leading to more precipitation over the Amazon but less precipitation over the major rainfall band located to the north of the Amazon. When the atmosphere over the Amazon is more stable in wet season, aerosols seem to reduce the precipitation over the region. Figure 7 illustrates the differences in the 850 hPa moisture flux and the vertically integrated moisture flux divergence between AERO and CTRL for October and December, respectively. It is shown that due to aerosol effect, stronger moisture divergence occurred over the major rainfall band (between 15°N and 5°S to the north of the Amazon) in October, while strengthened moisture convergence is produced over the Amazon. In December, anomalous divergence of moisture is produced over most area of the Amazon due to aerosol effect, leading to decreased precipitation.

To further delineate changes in circulation and relevant mechanisms caused by the aerosol forcing, we show the latitude-height cross sections of October temperatures and streamlines at 60°W for CTRL and the differences between AERO and CTRL (Fig. 8). In October which is

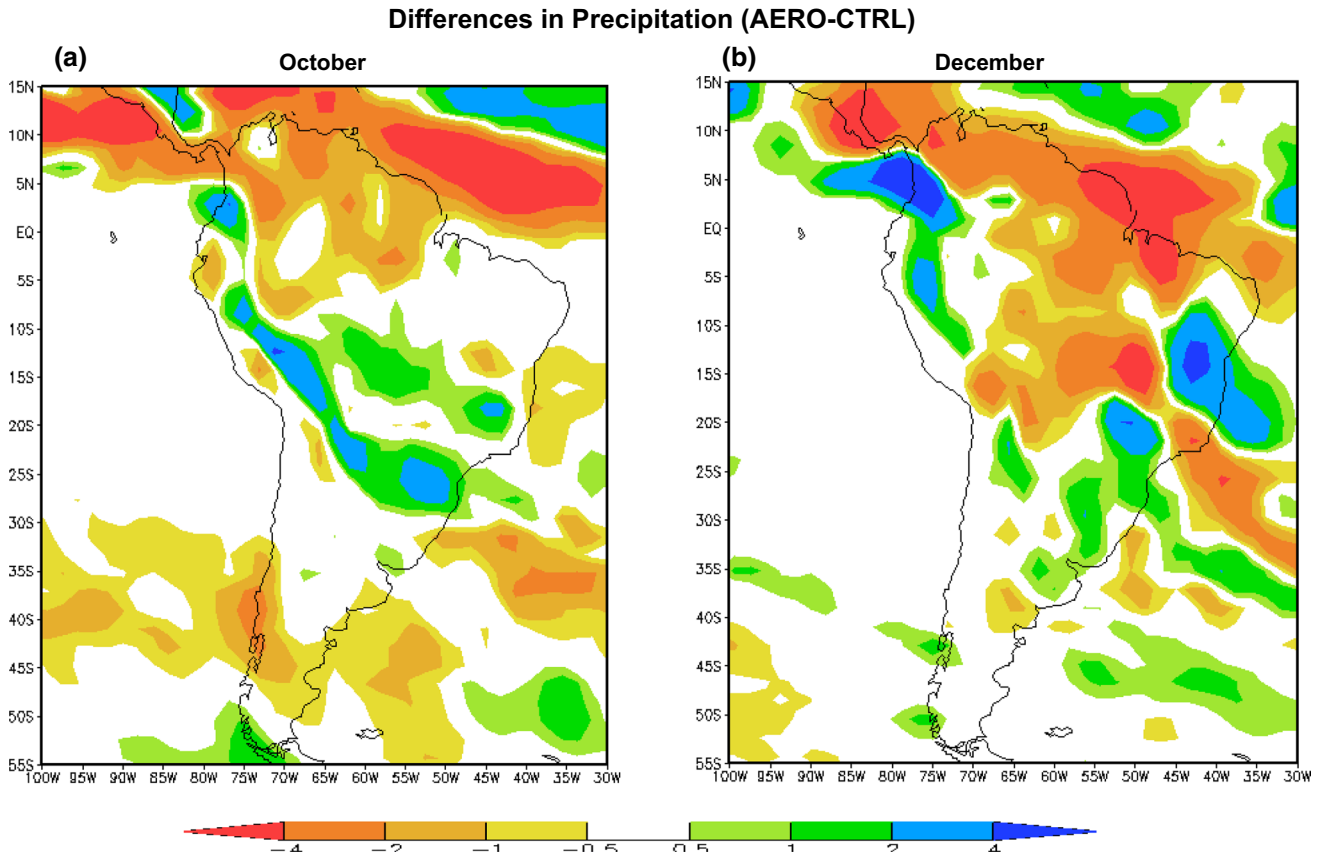

Fig. 6 Monthly mean precipitation (mm day^{-1}) differences between AERO and CTRL for **a** October and **b** December

the dry season, large scale upward motion is found over 15°N–10°S where the major rainfall is located. Another strong updraft region from surface is located over the Amazon (15°S–25°S) caused by the warmer land. The intersection of the deep tropical system (~15°N to 10°S) and the subtropical system to the south (~15°S to 25°S) results in a southward tilt of the stream lines in the middle troposphere (Fig. 8a). Aerosols are mostly located over the Amazon during October, leading to cooling over the Amazon and the area to its north, and warming to the south and the upper troposphere. The large scale surface cooling leads to the weakening of the upward motion and hence the reduced precipitation over the major rainfall band. Due to the rather strong subtropical convection over the Amazon, warming produced by the biomass burning aerosols occurs at the 200 hPa in the upper troposphere to the south of the Amazon, which induces anomalous updraft (Fig. 8b) and moisture convergence (Fig. 7a) around 20°S, resulting in increased precipitation over that region. This is in agreement with the elevated heat pump theory suggested by Lau et al. (2006) and also reported by Gu et al. (2006, 2016). In December, the large-scale upward motion shifts southward over 5°N–15°S, leading to the extension of the rainfall band to the Amazon. The monsoon inflow is seen near the surface at about 5°N and extends to about 15°S confined below 850 hPa, with ascending motion across these latitudes. The convection over 15°S–25°S becomes much shallower during the wet season, constrained by an anticyclonic circulation located at above 700 hPa (Fig. 9a). Due to the aerosol effects, cooling is found on the surface over 20°S–35°S, while warming is seen to the north in the entire air column and the south in the middle troposphere capped by the anticyclonic circulation, increasing the atmospheric stability. Anomalous downward motion is induced over 10°N–35°S, leading to a large area of reduced precipitation over the Amazon (Fig. 9b).

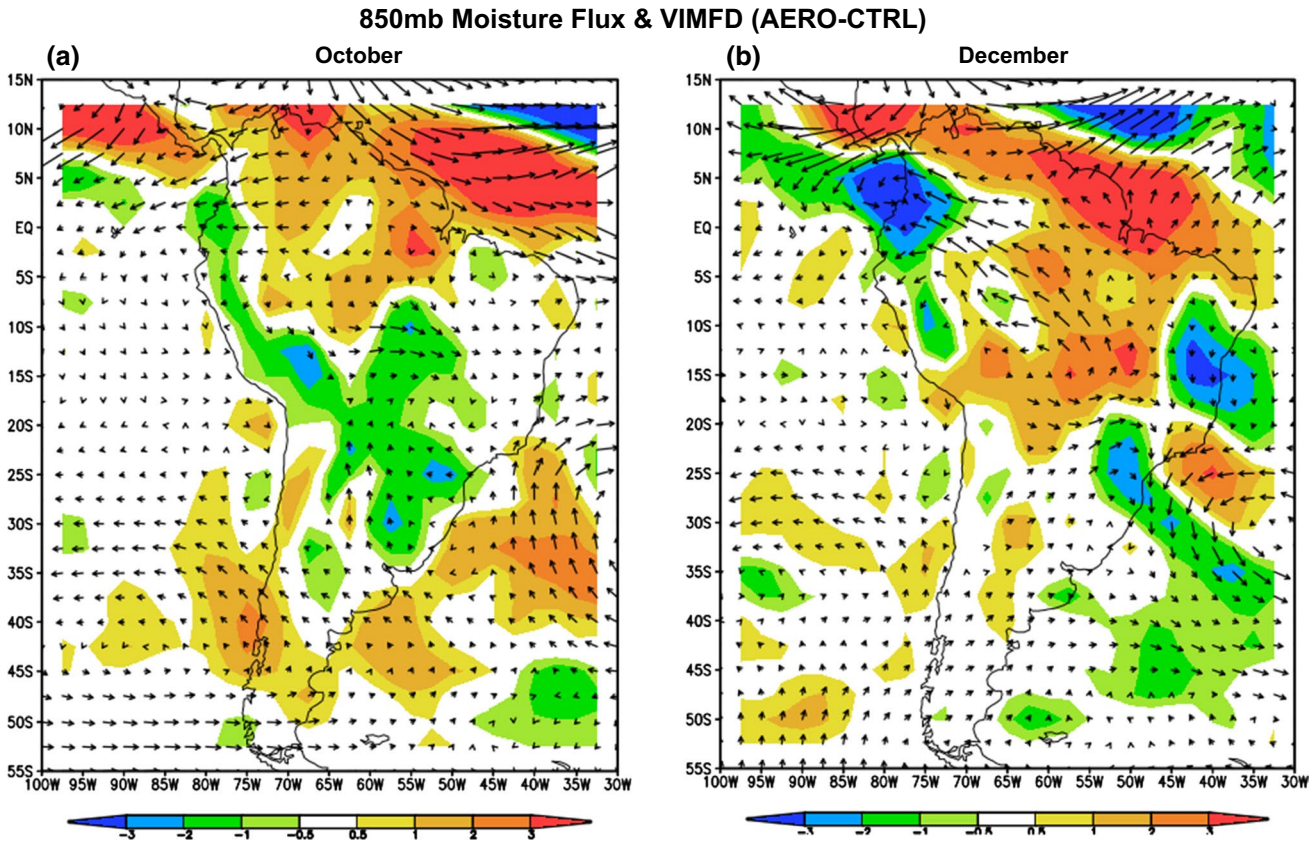

Fig. 7 Monthly mean differences in moisture flux (m s^{-1}) at 850 hPa and vertically integrated moisture flux divergence (mm day^{-1}) between AERO and CTRL for **a** October and **b** December

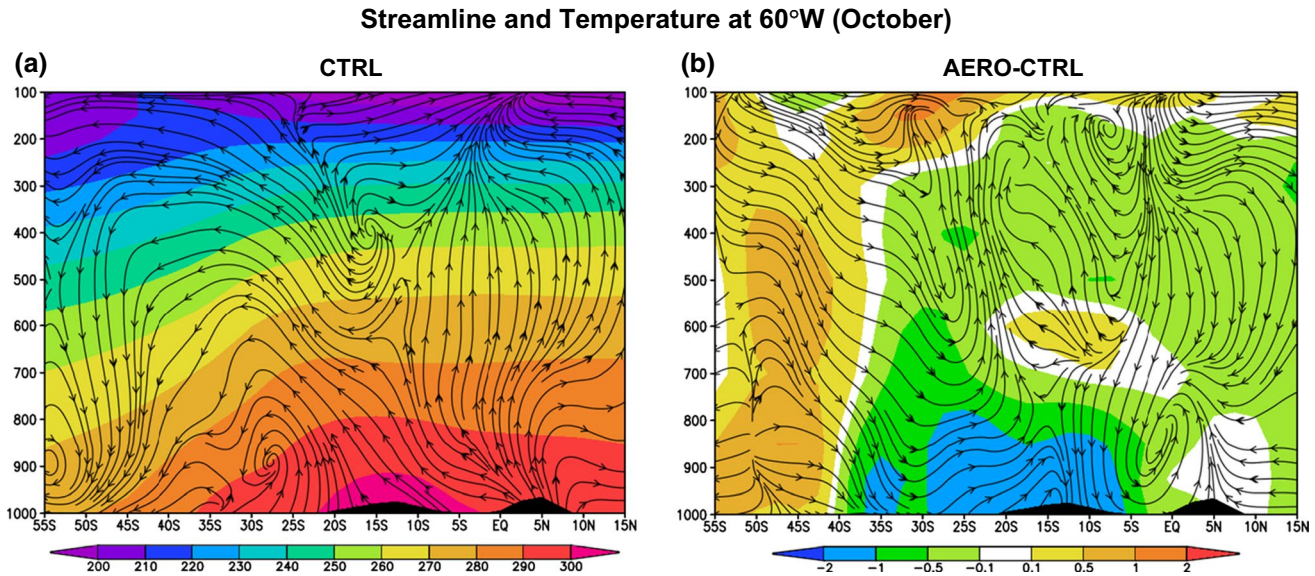

Fig. 8 Latitude-height cross section of October mean streamline (u; $-\omega \times 100$) and temperature (K, *shaded*) simulated from **a** CTRL and **b** differences between AERO and CTRL at 60°W

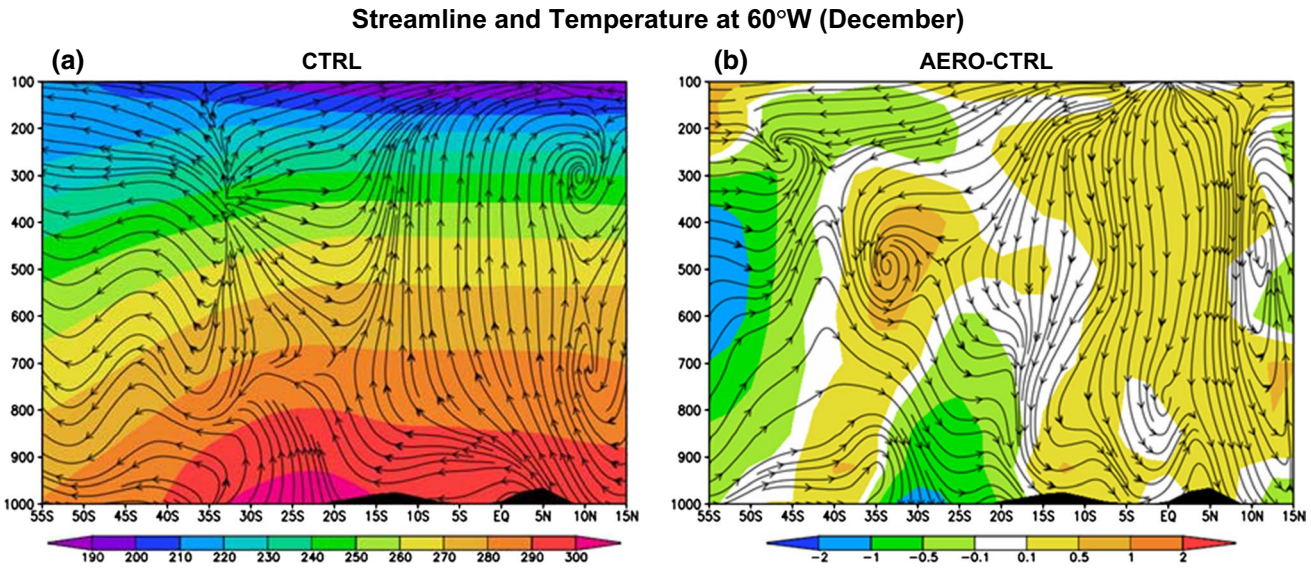

Fig. 9 Latitude-height cross section of December mean streamline (u; $-\omega \times 100$) and temperature (K, *shaded*) simulated from **a** CTRL and **b** differences between AERO and CTRL at 60°W

4 Conclusions

Climate simulations using the NCEP AGCM have been carried out to investigate the role of aerosols on regional climate, including surface temperature and precipitation as well as circulation during the dry to wet transition over the Amazon, with an emphasis on the evolution of precipitation. Two experiments have been performed, one with aerosol included, one without aerosol effect. The simulations consist of two sets of 6-year simulations with prescribed climatological SST and land processes, representing six members of each experiment starting from different initial conditions.

It is shown that with the inclusion of aerosols in the simulation, precipitation in the rainy season (DJF) decreases in this major rainfall band over the Amazon, which partially corrects the overestimate of the simulated precipitation in that region. In addition, simulation of precipitation distribution has also been improved for DJF by reducing the precipitation in the central and eastern Amazon while enhancing the rainfall in the western Amazon. Examination of the temporal revolution of monthly rainfall illustrates that during the late phase of dry season, the major rainfall band over 10°N to equator was weakened, while precipitation over the southern Amazon was enhanced due to aerosol effect. During the wet season, aerosol effect tends to delay the maximum precipitation over the Amazon by about half a month.

Aerosol effect is further investigated through the temporal evolution of zonally averaged differences in various fields. With aerosol effects included in the model, surface solar flux is reduced in the whole area due to the absorption and scattering of the solar radiation by aerosols, leading to decreased surface temperature. Sensible heat also decreases as a consequence of the cooler surface temperature, partially balancing the reduced surface solar radiation. Decrease in surface solar flux is also partially balanced by decreased latent heat flux which is a result of decreased precipitation in wet season. Precipitation generally decreases over the Amazon in the wet season but increases in March, indicating the delay of the wet season over the Amazon. Changes in cloud cover follow the patterns of precipitation evolution, as also indicated by the differences in OLR, an indication of convection strength.

Since the focus of this study is the aerosol effect during the transition period, simulation results for October (late phase of dry season) and December (early phase of wet season) have been further examined. During the dry season (October) when the atmosphere is more instable with a stronger convection, biomass burning aerosols produces warming over the 200 hPa in the upper troposphere, which induces an anomalous updraft around 20°S. Anomalous moisture convergence is produced over the Amazon while stronger moisture divergence occurs over the major rainfall band to the north of the Amazon. Precipitation is drawn further inland to the Amazon area, leading to more precipitation over the Amazon but less precipitation over the major tropical rainfall band. During the wet season (December) when the atmosphere is more stable with a much shallower convection over the Amazon, warming by aerosols mostly

occurs in the middle troposphere constrained by the anticyclonic circulation, while cooling occurs over the Amazon, leading to increased stability and anomalous downward motion. Consequently, strengthened divergence of moisture is produced over most area of the Amazon due to aerosol effect, leading to decreased precipitation. Therefore, roles of aerosols on precipitation over the Amazon during the dry to wet transition are different in association with the different characteristics of the regional atmospheric circulation patterns and stabilities.

Acknowledgments The authors appreciate the funding support by the GoAmazon project Award Number DE-SC0011117, NASA ROSES14-ACMAP programs, and NSF Grants AGS-1419526. Author J.H.J. also acknowledge the support from the NASA-sponsored Jet Propulsion Laboratory, California Institute of Technology.

References

Boisier JP, Ciais P, Ducharne A, Guibmerteau M (2015) Projected strengthening of Amazonian dry season by constrained climate model simulations. Nat Clim Change 5:656–660. doi:10.1038/nclimate2658

Butt N, de Oliveira PA, Costa MH (2011) Evidence that deforestation affects the onset of the rainy season in Rondonia, Brazil. J Geophys Res Atmos 116(D11):D11120. doi:10.1029/2010jd015174

Chou MD, Suarez MJ, Ho CH, Yan MMH, Lee KT (1998) Parameterizations for cloud overlapping and shortwave single-scattering properties for use in general circulation and cloud ensemble models. J Clim 11:202–214

Coakley JA, Cess RD, Yurevich FB (1983) The effect of tropospheric aerosols on the earth's radiation budget: a parameterization for climate models. J Atmos Sci 42:1408–1429

Cox PM, Harris PP, Huntingford C, Betts RA, Collins M, Jones CD, Jupp TE, Marengo JA, Nobre CA (2008) Increasing risk of Amazonian drought due to decreasing aerosol pollution. Nature 453(7192):212–215

Fels SB, Schwarzkopf MD (1975) The simplified exchange approximation: a new method for radiative transfer calculations. J Atmos Sci 32:1475–1488

Fu R, Li W (2004) The influence of the land surface on the transition from dry to wet season in Amazonia. Theor Appl Climatol 78:97–110. doi:10.1007/s00704-004-0046-7

Fu R, Dickinson RE, Chen M, Wang H (2001) How do tropical sea surface temperatures influence the seasonal distribution of precipitation in the equatorial Amazon? J Clim 14(20):4003–4026. doi:10.1175/1520-0442(2001)014<4003:hdtsst>2.0.co;2

Goncalves WA, Machado LAT, Kirstetter PE (2015) Influence of biomass aerosol on precipitation over the Central Amazon: an observational study. Atmos Chem Phys 15:6789–6800. doi:10.5194/acp-15-6789-2015

Greco S, Swap R, Garstang M, Ulanski S, Shipham M, Harriss RC, Talbot R, Andreae MO, Artaxo P (1990) Rainfall and surface kinematic conditions over central Amazonia during ABLE 2B. J Geophys Res Atmos 95(D10):17001–17014. doi:10.1029/JD095iD10p17001

Gu Y, Liou KN, Xue Y, Mechoso CR, Li W, Luo Y (2006) Climatic effects of different aerosol types in China simulated by the UCLA general circulation model. J Geophys Res 111:D15201. doi:10.1029/2005JD006312

Gu Y, Liou KN, Chen W, Liao H (2010) Direct climate effect of black carbon in China and its impact on dust storm. J Geophys Res 115:D00K14. doi:10.1029/2009JD013427

Gu Y, Liou KN, Jiang JH, Su H, Liu X (2012) Dust aerosol impact on North Africa climate: a GCM investigation of aerosol-cloud-radiation interactions using A-Train satellite data. Atmos Chem Phys 12:1667–1679. doi:10.5194/acp-12-1667-2012

Gu Y, Xue Y, De Sales F, Liou KN (2016) A GCM investigation of dust aerosol impact on the regional climate of North Africa and South/East Asia. Clim Dyn 46:2353–2370. doi:10.1007/s00382-015-2706-y

Hansen J, Sato M, Ruedy R (1997) Radiative forcing and climate response. J Geophys Res 102:6831–6864

Hess M, Koepke P, Schult I (1998) Optical properties of aerosols and clouds: the software package OPAC. Bull Am Meteorol Soc 79:831–844

Heymsfield AJ, McFarquhar GM (1996) High albedos of cirrus in the tropical Pacific warm pool. J Atmos Sci 53:2424–2451

Hou YT, Campana KA, Yang SK (1996) Shortwave radiation calculations in the NCEP's global model. In: International radiation symposium, IRS-96, August 19–24, Fairbanks, AL

Hou YT, Moorthi S, Campana KA (2002) Parameterization of solar radiation transfer in the NCEP models. NCEP Office Note, 441. http://www.emc.ncep.noaa.gov/officenotes/FullTOC.html#2000

Jiang JH, Su H, Schoeberl M, Massie ST, Colarco P, Platnick S, Livesey N (2008) Clean and polluted clouds: relationships among pollution, ice cloud and precipitation in South America. Geophys Res Lett 35:L14804. doi:10.1029/2008GL034631

Jiang JH, Su H, Zhai C, Massie ST, Schoeberl MR, Colarco PR, Platnick S, Gu Y, Liou KN (2011) Influence of convection and aerosol pollution on ice cloud particle effective radius. Atmos Chem Phys 11:457–463. doi:10.5194/acp-11-457-2011

Johnson BT, Shine K, Forster P (2004) The semi-direct aerosol effect: impact of absorbing aerosols on marine stratocumulus. Q J R Meteorol Soc 130:1407–1422

Joseph JH, Wiscombe WJ, Weinman JA (1976) The delta-Eddington approximation for radiative flux transfer. J Atmos Sci 33:2452–2459

Kanamitsu M, Ebisuzaki W, Woollen J, Yang SK, Hnilo JJ, Fiorino M, Potter GL (2002) NCEP-DOE AMIP-II Reanalysis (R-2). Bull Am Meteorol Soc 83:1631–1643

Kiehl JT, Hack JJ, Bonan GB, Boville BA, Williamson DL, Rasch PJ (1998) The national center for atmospheric research community climate model: CCM3. J Clim 11:1131–1149

Lau KM, Kim MK, Kim KM (2006) Asian summer monsoon anomalies induced by aerosol direct forcing: the role of the Tibetan Plateau. Clim Dyn 26:855–864. doi:10.1007/s00382-006-0114-z

Lenters JD, Cook KH (1997) On the origin of the Bolivian high and related circulation features of the South American climate. J Atmos Sci 54:22

Lewis SL, Brando PM, Phillips OL, van der Heijden GMF, Nepstad D (2011) The 2010 Amazon drought. Science 331:6017. doi:10.1126/science.1200807

Li W, Fu R (2004) Transition of the large-scale atmospheric and land surface conditions from the dry to the wet season over Amazonia as diagnosed by the ECMWF re-analysis. J Clim 17:2637–2651

Liebmann B, Marengo JA (2001) Interannual variability of the rainy season and rainfall in the Brazilian Amazon Basin. J Clim 14:4308–4318

Machado LAT, Rossow WB, Guedes RL, Walker AW (1998) Life cycle variations of mesoscale convective systems over the Americas. Mon Weather Rev 126(6):1630–1654. doi:10.1175/1520-0493(1998)126<1630:lcvomc>2.0.co;2

Marengo JA, Nobre CA, Tomasella J, Oyama MD, Sampaio de Oliveira G, de Oliveira R, Camargo H, Alves LM, Brown IF

(2008) The drought of Amazonia in 2005. J Clim 21(3):495–516. doi:10.1175/2007jcli1600.1

Marengo JA, Tomasella J, Alves LM, Soares WR, Rodriguez DA (2011) The drought of 2010 in the context of historical droughts in the Amazon region. Geophys Res Lett. doi:10.1029/2011gl047436

Martin ST, Andreae MO, Artaxo P, Baumgardner D, Chen Q, Goldstein AH, Guenther A, Heald CL, Mayol Bracero OL, McMurry PH, Pauliquevis T, Poschl U, Prather KA, Roberts GC, Saleska SR, Silva Dias MA, Spracklen DV, Swietlicki E, Trebs I (2010) Sources and proprieties of Amazonian aerosol particles. Rev Geophys 48(1–42):RG000280. doi:10.1029/2008RG000280

Martins JA, Silva Dias MAF, Gonçalves FLT (2009) Impact of biomass burning aerosols on precipitation in the Amazon: a modeling case study. J Geophys Res 114:D02207. doi:10.1029/2007JD009587

Menon S, Hansen J, Nazarenko L, Luo Y (2002) Climate effects of black carbon aerosols in China and India. Science 297:2250–2253

Miller RL, Tegen I (1998) Climate response to soil dust aerosols. J Clim 11:3247–3267

Pan HL, Wu WS (1995) Implementing a mass flux convective parameterization package for the NMC medium-range forecast model. NMC Off Note 409, pp 40

Petersen WA, Nesbitt SW, Blakeslee RJ, Cifelli R, Hein P, Rutledge SA (2002) TRMM observations of intraseasonal variability in convective regimes over the Amazon. J Clim 15(11):1278–1294. doi:10.1175/1520--0442(2002)015<1278:tooivi>2.0.co;2

Petersen WA, Fu R, Chen M, Blakeslee R (2006) Intraseasonal forcing of convective and lightning activity in the southern Amazon as a function of cross-equatorial flow. J Clim 19:3180–3196

Rickenbach TM (2002) Modulation of convection in the southwestern Amazon basin by extratropical stationary fronts. J Geophys Res. doi:10.1029/2000jd000263

Schwarzkopf MD, Fels SB (1991) The simplified exchange method revisited: an accurate, rapid method for computation of infrared cooling rates and fluxes. J Geophys Res 96(D5):9075–9096

Silva Dias MAF (2002) Cloud and rain processes in a biosphere–atmosphere interaction context in the Amazon Region. J Geophys Res. doi:10.1029/2001jd000335

Sundqvist H, Berge E, Kristjansson JE (1989) Condensation and cloud studies with mesoscale numerical weather prediction model. Mon Weather Rev 117:1641–1757

Xie P, Arkin PA (1997) Global precipitation: a 17-year monthly analysis based on gauge observations, satellite estimates and numerical model outputs. Bull Am Meteorol Soc 78:2539–2558

Xu KM, Randall DA (1996) A semi-empirical cloudiness parameterization for use in climate models. J Atmos Sci 53:3084–3102

Xue Y, Sellers PJ, Kinter JL III, Shukla J (1991) A simplified biosphere model for global climate studies. J Clim 4:345–364

Xue Y, Juang HMH, Li WP, Prince S, DeFries R, Jiao Y, Vasic R (2004) Role pf land surface processes in monsoon development: East Asia and West Africa. J Geophys Res 109:D03105. doi:10.1029/2003JD003556

Zeng N, Yoon J-H, Marengo JA, Subramaniam A, Nobre CA, Mariotti A, Neelin JD (2008) Causes and impacts of the 2005 Amazon drought. Environ Res Lett 3(1):014002

Zhan X, Xue Y, Collatz GJ (2003) An analytical approach for estimating CO2 and heat fluxes over the Amazonian region. Ecol Model 162:97–117

Zhao QY, Carr FH (1997) A prognostic cloud scheme for operational NWP models. Mon Weather Rev 125:1931–1953